

Improved microwave shielding properties of polyaniline grown over three-dimensional hybrid carbon assemblage substrate

Ashok K. Sharma · Preetam Bhardwaj ·
Kamal Kant Singh · Sundeep K. Dhawan

Received: 26 August 2014 / Accepted: 17 September 2014 / Published online: 27 September 2014
© The Author(s) 2014. This article is published with open access at Springerlink.com

Abstract Novel composites were prepared by oxidative polymerization of aniline over hybrid carbon nanostructured assemblage consisting of graphene and amine functionalized multiwalled carbon nanotubes. The chemical structure of the obtained composites has been confirmed by UV–visible Spectroscopy and Fourier transform infrared spectroscopy. To know about the crystalline properties of the composites, X-ray diffraction studies have been done. The structural and morphological properties of the composites were examined by scanning electron microscopy. The composite having thinnest polymer film exhibited highest conductivity of 0.11 S/cm and maximum electromagnetic interference shielding effectiveness value of 21 dB obtained in the frequency range 12–18 GHz (KU-band).

Keywords Amine functionalised CNTs · Graphene · Polyaniline · Composites · Microwave shielding

Introduction

Electromagnetic interference (EMI) is a well-known problem in electronic instruments, radar and antenna systems and military electronic devices. EMI is an unwanted electromagnetic wave that acts as a noise to electronic devices, perturbing their operation. This noise originates from natural phenomenon such as thunder, solar flare and

electrostatic discharge (ESD). It also comes from other electronic devices that emit electromagnetic waves. There is a critical need for developing effective and practical EMI shielding materials and their potential applications. Electromagnetic (EM) radiation takes the form of self-propagating waves in a vacuum or in matter. These EM waves are classified according to their frequency and are called radio frequency (RF) waves, microwaves, millimeter waves, terahertz radiation, infrared radiation, visible light, ultraviolet radiation, X-rays and Gamma rays. For wireless terrestrial communication, RF and the lower end of microwave transmission are being heavily used. Thus, the importance of EMI shielding materials to isolate electronic devices from noises cannot be neglected. Today shielding against EMI is practiced by government, military, medical, private industries and R & D laboratories. The importance of EMI shielding relates the high demand of speedy communication and reliability of electronic equipment, digital devices and wireless technology. Shielding is considered acceptable if it attenuates the intensity of electromagnetic field to an adequate level established by regulation of the electronic devices. It is also needed for deterring electromagnetic form of spying. It is, therefore, vital to develop new materials with enhanced EMI shielding capacity. It is well known that the shield should be conducting; therefore, usually the shielding techniques focus on the use of standard metals and their composites which have shortcomings of limited mechanical flexibility, heavy weight, corrosion, physical rigidity and difficulty in tuning the shielding efficiency (Saini et al. 2009; Singh et al. 2013; Pande et al. 2009; Qin et al. 2010). Further, metals mainly reflect the radiation and cannot be used in applications where absorption is the prime requisite.

In the past four decades, conducting polymers (CPs) have gained a special status owing to wealth of applications

A. K. Sharma (✉) · P. Bhardwaj · K. K. Singh
Department of Materials Science and Nanotechnology,
D.C.R. University of Science and Technology, Murthal, India
e-mail: aksharma210@gmail.com

P. Bhardwaj · S. K. Dhawan
Conducting Polymers Group, CSIR-National Physical
Laboratory, New Delhi, India

(Olmedo et al. 2001; Sharma and Sharma 2012; Sharma and Shukla 2013; Saini et al. 2009). The EMI shielding and microwave absorption properties of these polymers can be explained in terms of electrical conductivity and presence of bound/localized charges (polarons/bipolarons) leading to strong polarization and relaxation effects.

Polyaniline (PANI) has special status among other conducting polymers due to its non-redox doping, good environmental stability and economic feasibility. The properties can be further tuned by controlled polymerization conditions and using substituted anilines, specific comonomers, dopants and fillers. PANI has low inherent specific strength and requires dispersion in some binding matrix to form composites for any commercially useful product (Sharma and Sharma 2012; Saini et al. 2009).

Graphene and carbon nanotubes have attracted much attention due to their unusual two- and one-dimensional structure with novel properties. With potential applications ranging from molecular electronics and field-emission displays to nanocomposites, graphene and carbon nanotubes (CNTs) offer tremendous opportunity in the development of multi-functional material systems. Exceedingly high electronic properties of the graphene and carbon nanotubes have attracted attention for the development of super conducting light weight structures. The combination of Graphene and CNTs become a three-dimensional structure that is a suitable substrate for the growth of a conducting polymer. Since their discovery, the exceptional mechanical, electrical and thermal properties of carbon nanotube (Iijima and Ichihashi 1993) and graphene (Novoselov et al. 2005, Meyer et al. 2007, Das and Prusty 2013) made them potential candidate for high-tech applications. On account of various tremendous properties of conducting polymers, CNTs and graphene, it is reasonable to develop a nanostructure hybrid composite so that the properties of the materials can be enhanced and the composite can be used for advanced applications. The authors Gupta et al. (2014), Saini et al. (2009), Singh et al. (2013) and Pande et al. (2009) reported the EMI shielding properties with the variations in the filler loadings (MWCNTs and graphene), whereas, in this work, we investigated the effect on conductivity and EMI shielding properties of the composite materials obtained by varying the mole content of aniline monomer in the initial polymerization solution.

Experimental

Materials

Aniline (99 %), and Ammonium per sulfate [APS, $(\text{NH}_4)_2\text{S}_2\text{O}_8$, 98 %], were purchased from Sigma Aldrich, Germany. Amine functionalized multiwalled carbon

nanotubes (nanocyl, Belgium) and graphene (XG Sciences, United States) were used as such without any purification. All other chemicals like hydrochloric acid and methanol were used as received and were of analytical grade. Solutions were prepared in deionized water. Aniline was vacuum distilled before use.

Synthesis of polyaniline-hybrid carbon assemblage based composites

Equally weighed amounts of amine functionalized MWCNTs and graphene (0.1 g) were ultrasonicated for 2 h in 20 % aqueous methanol solution for preparing hybrid carbon assemblage. The monomer solution of aniline (0.02, 0.05, 0.1, 0.2 M) was added to dispersed hybrid carbon assemblage. Oxidant solution of ammonium per sulfate (APS) was added dropwise to the filler and matrix phase solutions. The mixture was left for polymerization at 0–5 °C for 6 h with constant stirring. The polyaniline-hybrid carbon assemblage based composites were obtained by filtering and rinsing of the reaction mixture with deionized water and methanol, followed by drying of the remaining powder under vacuum at 60 °C for 24 h. Methanol washing is desirable to remove the oligomeric impurities.

Characterization

Infrared spectrum (KBr pellet) was recorded using Fourier transform infrared spectrophotometer (Perkin Elmer spectrum BXII FTIR) and electron microscopy (SEM, JEOL-JSM-5600LV @ accelerating voltage 20kv) was used to examine the surface morphology of graphene, amine functionalized CNTs (AMWCNTs) and Polyaniline-hybrid carbon assemblage composites. The ordered structures of composites were studied by XRD. X-ray diffraction data were obtained on a Philips (Xpert PRO) machine using $\text{CuK}\alpha$ source and fitted with an X'celerator detector (PW 3,050/60). Data were collected at 2θ with varying intensity. The diffractogram was in terms of 2θ in the range 5°–80°. UV–Vis absorption measurements were performed in the range 200–800 nm using standard spectrometer (Perkin-Elmer, Lambda-45). The electrical conductivity of the composite samples was measured by 4-probe method. For this, the polymer composite sample was in rectangular strip of size 30 mm in length and 10 mm in width. The rectangular strips of composite samples were made using a rectangular die set and a pelletizer compressed at 60 MPa. The current was passed along the length of the strip and the voltage drop was measured across different points separated by unit length. Each sample reading was averaged over 10–15 readings. The room temperature current–voltage (I – V) characteristics were measured and resistance

values were obtained from the slope of these plots. Keithley 224 programmable current source was used for providing current. The voltage drop was measured by Keithley 197A auto ranging micro volt DMM. The EMI shielding effectiveness measurements of the composites were carried out on an Agilent E8362B vector network analyzer in the frequency range of 12.4–18 GHz (Ku Band).

Results and discussion

Physicochemical studies of composites by FTIR-spectroscopy

Figure 1 shows the FTIR spectra of PANI, hybrid carbon assemblage and the composite. In hybrid carbon assemblage spectra, the peak at $3,420\text{ cm}^{-1}$ corresponds to the NH_2 stretching. The peak at $1,632\text{ cm}^{-1}$ corresponded to the N–H bending of amine. Further, the peaks at $1,124$ and $1,010\text{ cm}^{-1}$ are attributed to C–C stretch vibration of main structure of MWCNTs and graphene. The peaks at $1,218$ and $1,417\text{ cm}^{-1}$ are ascribed to C–N stretching of amide groups. The $3,420\text{ cm}^{-1}$ peak is produced by the flexible fluctuation of primary amine that ensures the presence of amine group in amine functionalized MWCNTs (Sharma and Shukla 2013). For polyaniline, the peaks near $1,560$ and $1,480\text{ cm}^{-1}$ are characteristic stretching bands of nitrogen quinoid (N–Q–N) and benzenoid (N–B–N) (Sharma and Sharma 2012; Sharma and Shukla 2013; Saini et al. 2009). These are due to the conducting state of the polymer. The prominent peak around $1,120\text{ cm}^{-1}$ (C–N stretching) is due to the charge delocalization over the polymeric backbone (Ozkazanca et al 2012; Saini et al. 2009). The band around 858 cm^{-1} is due to the out of the plane C–H bending vibrations. The prominent peak at $3,438\text{ cm}^{-1}$ was observed due to NH_2 stretching vibrations (Sharma and Sharma 2012). A slight shift was observed in the position of the main characteristic peaks in composite spectrum, which indicates interaction of hybrid carbon assemblage with PANI. The increase in the relative intensity of peaks around $3,438$, $1,480$ and $1,120\text{ cm}^{-1}$ may be attributed to the PANI attached to hybrid carbon assemblage.

UV–vis studies

UV–vis spectra of PANI, hybrid carbon assemblage and composite are given in Fig. 2. In hybrid carbon assemblage, presence of graphene and amine functionalized MWCNTs show a broad peak between 200 and 320 nm centered at 260 nm which is attributed to π – π^* electron transition (Yang et al. 2009). The absorption peak at 213 nm can be ascribed to C–N bonding of the amide group formed

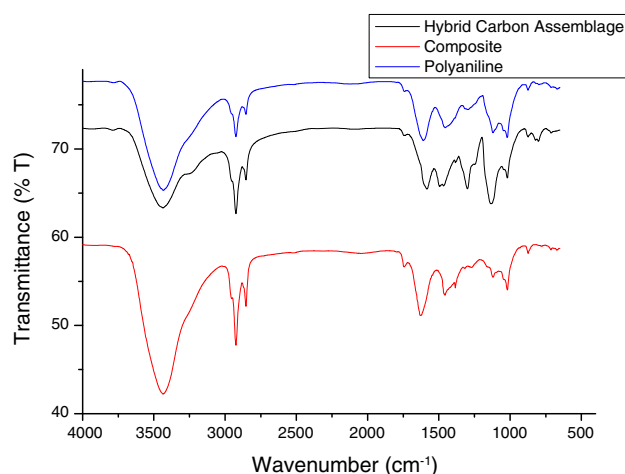


Fig. 1 FTIR spectra of polyaniline, hybrid carbon assemblage and composite

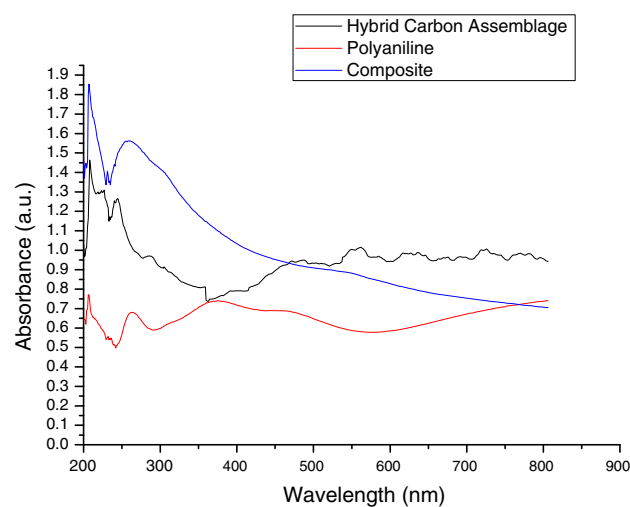


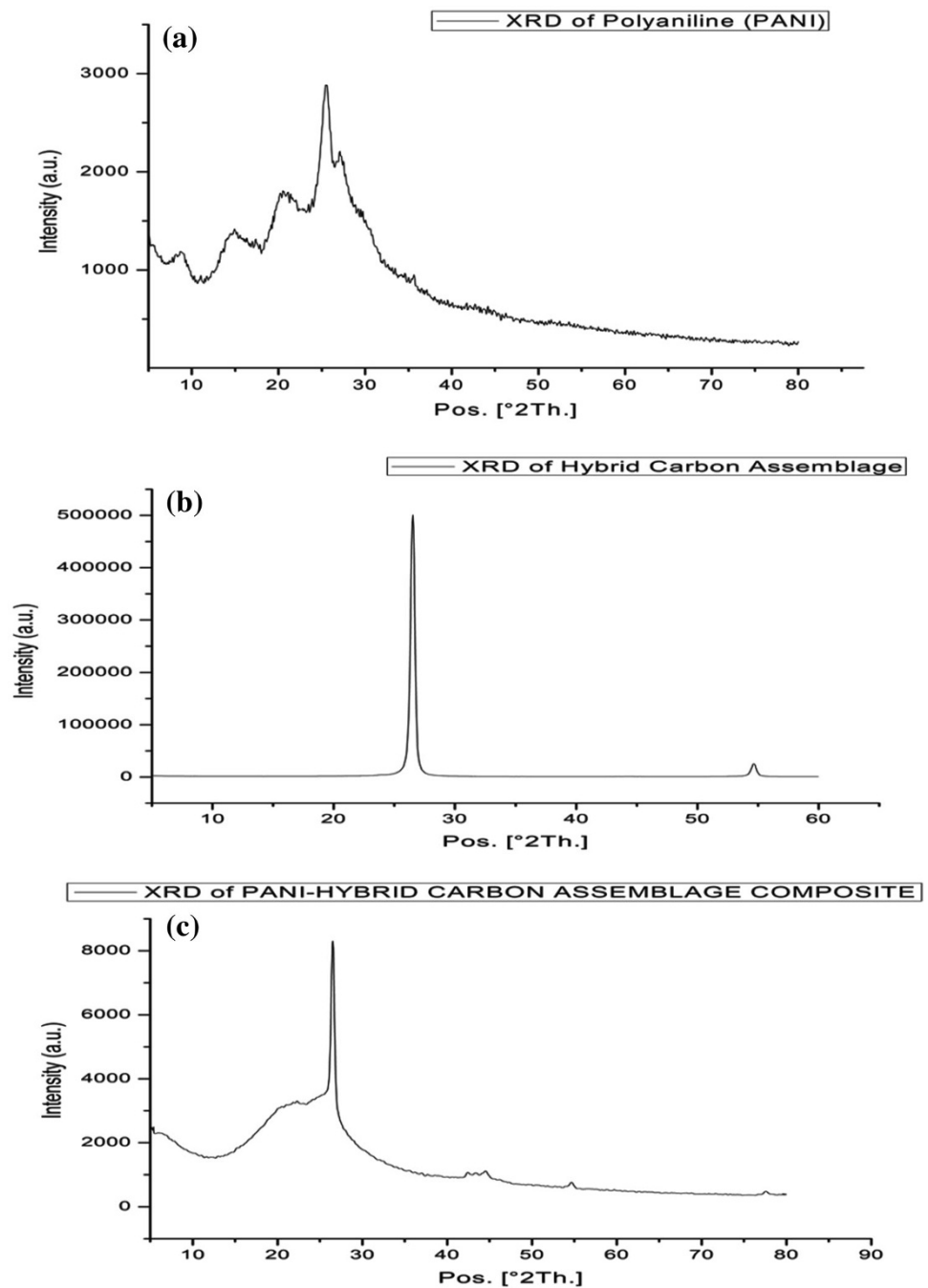
Fig. 2 UV-vis spectra of polyaniline, hybrid carbon assemblage and composite

due to presence of amine functionalized CNTs (Jimeno et al. 2009). For PANI, the absorption band at 300–350 nm shows π – π^* transitions of benzenoid rings. The band at 400–450 nm shows polaron– π^* transitions and the band at 500–700 nm shows π – π^* transitions of quinone-imine groups. All these absorption bands seen in UV–vis spectra of PANI and composite belong to the characteristic emeraldine salt form of PANI (Ozkazanca et al. 2012). Both FTIR and UV–vis spectra clearly indicate that PANI and its composite, which were chemically synthesized in this study are in electrically conductive emeraldine salt form.

X-Ray diffraction pattern

Figure 3 represents the XRD patterns of hybrid carbon assemblage, PANI and PANI–hybrid carbon assemblage

Fig. 3 XRD pattern of **a** polyaniline, **b** hybrid carbon assemblage and **c** composite



composite. The hybrid carbon assemblage shows a sharp peak centered on 2θ value of 26° which corresponds to the (0 0 2) planes of MWCNT and graphene. The peak around 54° is due to the graphitic plane. The characteristic peaks of the PANI are observed around 2θ values of 15° , 20° , 25° (Sharma and Sharma 2012) corresponding to (0 1 1), (0 2 0), (2 0 0) (Saini et al. 2009) reflections of emeraldine without any additional bands indicating absence of covalent interactions between the PANI and assemblage. In composite spectra, the slight shifting in the peak positions may be ascribed to charge transfer interactions between

PANI and hybrid carbon assemblage leading to variations in chain packing and configurations. The composite shows the characteristic peaks of both PANI and hybrid carbon assemblage.

Morphology of composites

SEM micrographs of the amine functionalized multiwalled carbon nanotubes and graphene and are shown in Fig. 4a, b respectively. It is observed that graphene is two-dimensional sheets of carbon atoms and AMWCNTs are hollow

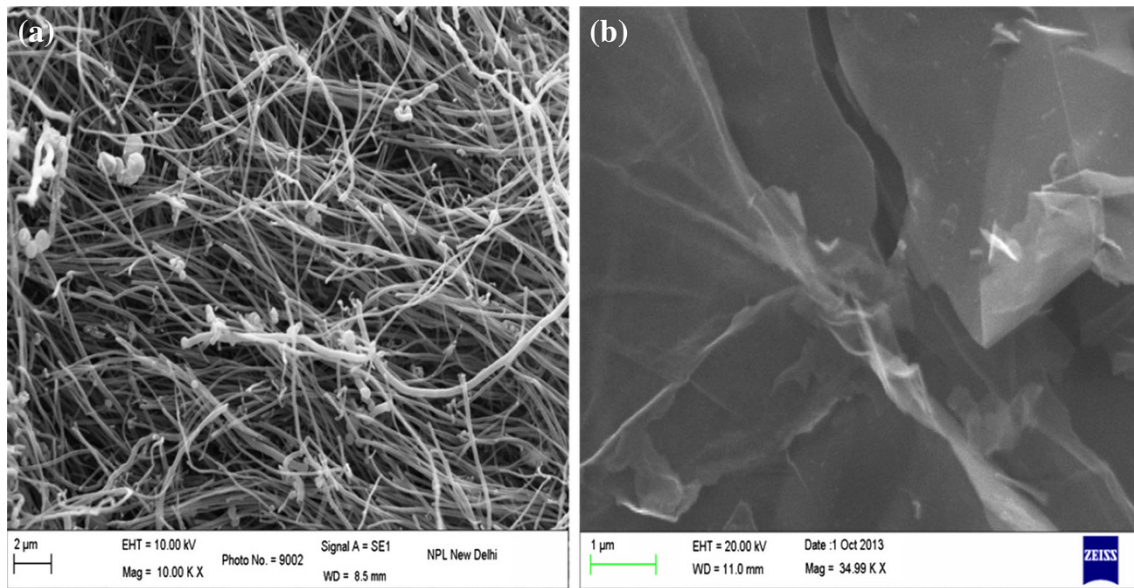


Fig. 4 SEM micrographs of **a** AMWCNTs and **b** graphene

cylindrical shaped tubes structure of carbon atoms. Figure 5a–e represents SEM morphology of PANI and composites with different monomer concentrations. PANI shows rough, smooth and flaky surfaces. From Fig. 5b–e, it has been observed that there is increase in degree of roughness and agglomeration in morphology of composites with increase in aniline monomer concentration. The morphology of the composite having highest monomer content (Fig. 5e) showed the formation of rough and highly aggregated globules. This result indicates that higher concentration of the monomer in the initial polymerization solution results in increased polymerization rate, leading to rough surface and poor adhesion film. This poor adhesion film causes increase in contact resistance between hybrid carbon assemblage substrate and PANI. However, the composite of lower monomer concentration (02PANI-HY-C) does not possess any aggregated globular morphology (Fig. 5b). This suggested the formation of good adhesive polymeric film over three-dimensional hybrid carbon assemblage supported by the fact that the composite 02PANI-HY-C had highest conductivity (Fig. 6).

Conductivity measurements

The electrical conductivities of the PANI and the hybrid assemblage composites were calculated by considering the sample dimensions as

$$\sigma = \frac{L}{RA},$$

where “ L ” is the length of the composites “ R ” is resistance and “ A ” is cross-sectional area of the composite normal to

direction of current flow. The measured conductivity of PANI was found to be 0.0092 S/cm. The conductivity of various composites v/s the molar concentrations is shown in the Fig. 6. The composite having thinnest PANI film, 02PANI-HY-C, exhibited highest conductivity of 0.11 S/cm. Therefore, by incorporating the polyaniline on to the hybrid carbon assemblage, there is increment in conductivity by 2 orders in comparison to the PANI alone which is indicative of synergy effect in the obtained composite materials.

EMI shielding effectiveness measurement

EMI shielding was measured on rectangular strips of composites inside the sample holder. The holder matches the internal dimensions of Ku band (12.4–18 GHz) waveguide placed between the two ports of Vector Network Analyzer (VNA E8263B Agilent Technologies). The EMI shielding is a direct result of reflection, absorption and multiple internal reflection losses at the existing interfaces, suffered by incident electromagnetic (EM) waves. EMI shielding effectiveness can be expressed as (Das et al. 2000; Saini et al. 2009, 2011; Singh et al. 2013) follows:

$$SE_T(\text{dB}) = 10 \log \left[\frac{P_T}{P_I} \right] = 20 \log \left[\frac{E_T}{E_I} \right] = 20 \log \left[\frac{H_T}{H_I} \right], \quad (1)$$

where P_I (E_I or H_I) and P_T (E_T or H_T) are the incident and transmitted electromagnetic powers (electric or magnetic field), respectively. The total shielding effectiveness can further be divided into three components:

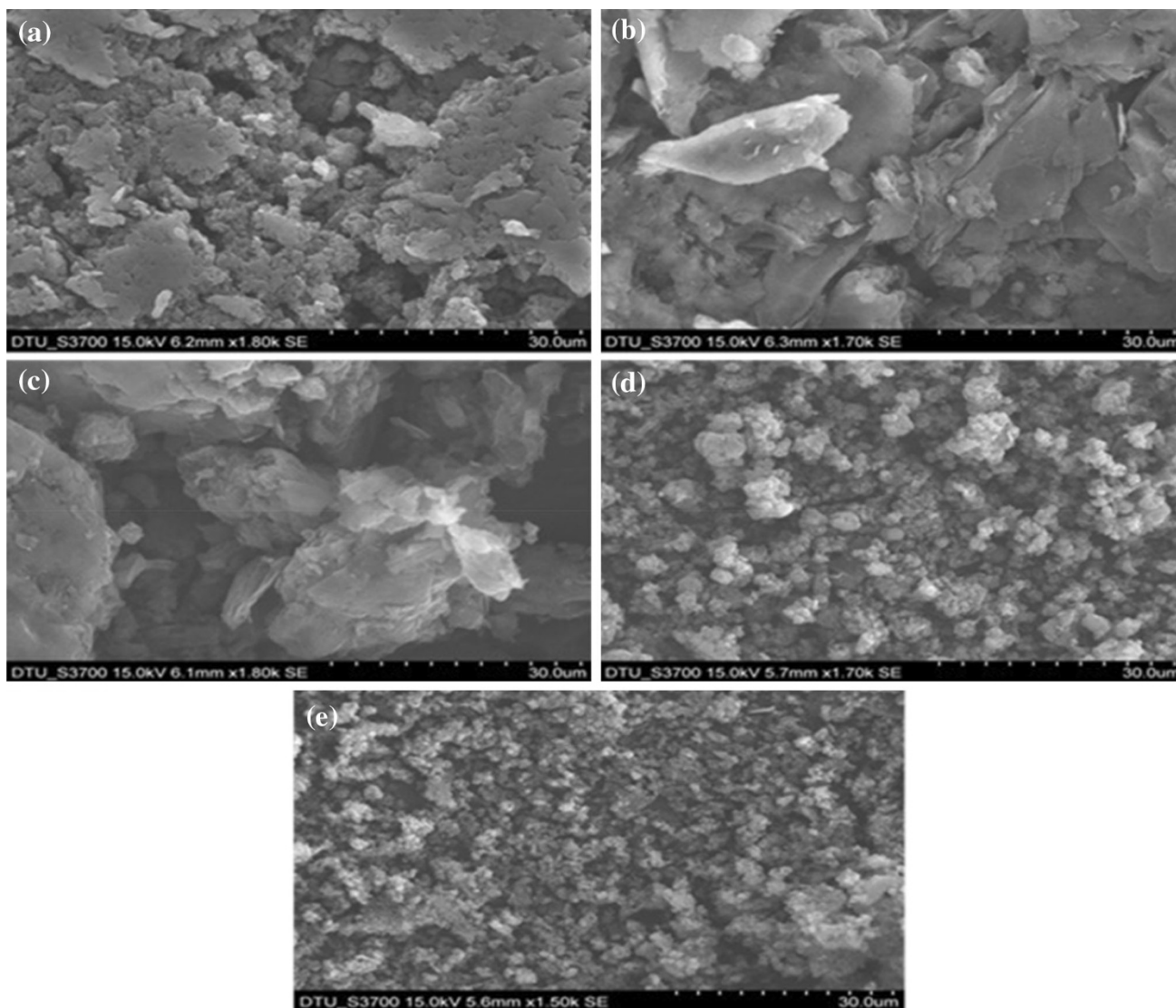


Fig. 5 SEM micrographs of **a** PANI, **b** 0.02M PANI-HY-C, **c** 0.05M PANI-HY-C, **d** 0.1M PANI-HY-C and **e** 0.2M PANI-HY-C

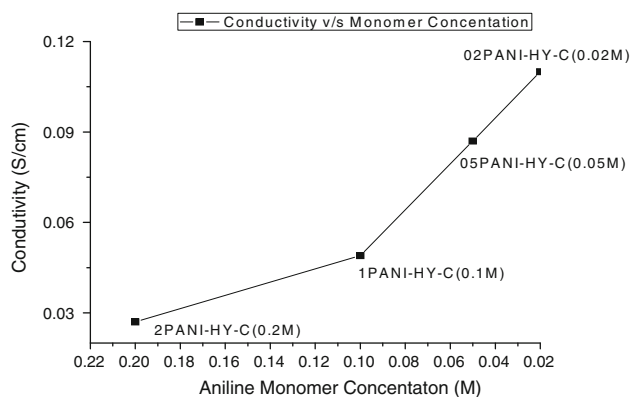


Fig. 6 Plot of conductivities of various composites

$$SE_T = SE_R + SE_A + SE_M, \quad (2)$$

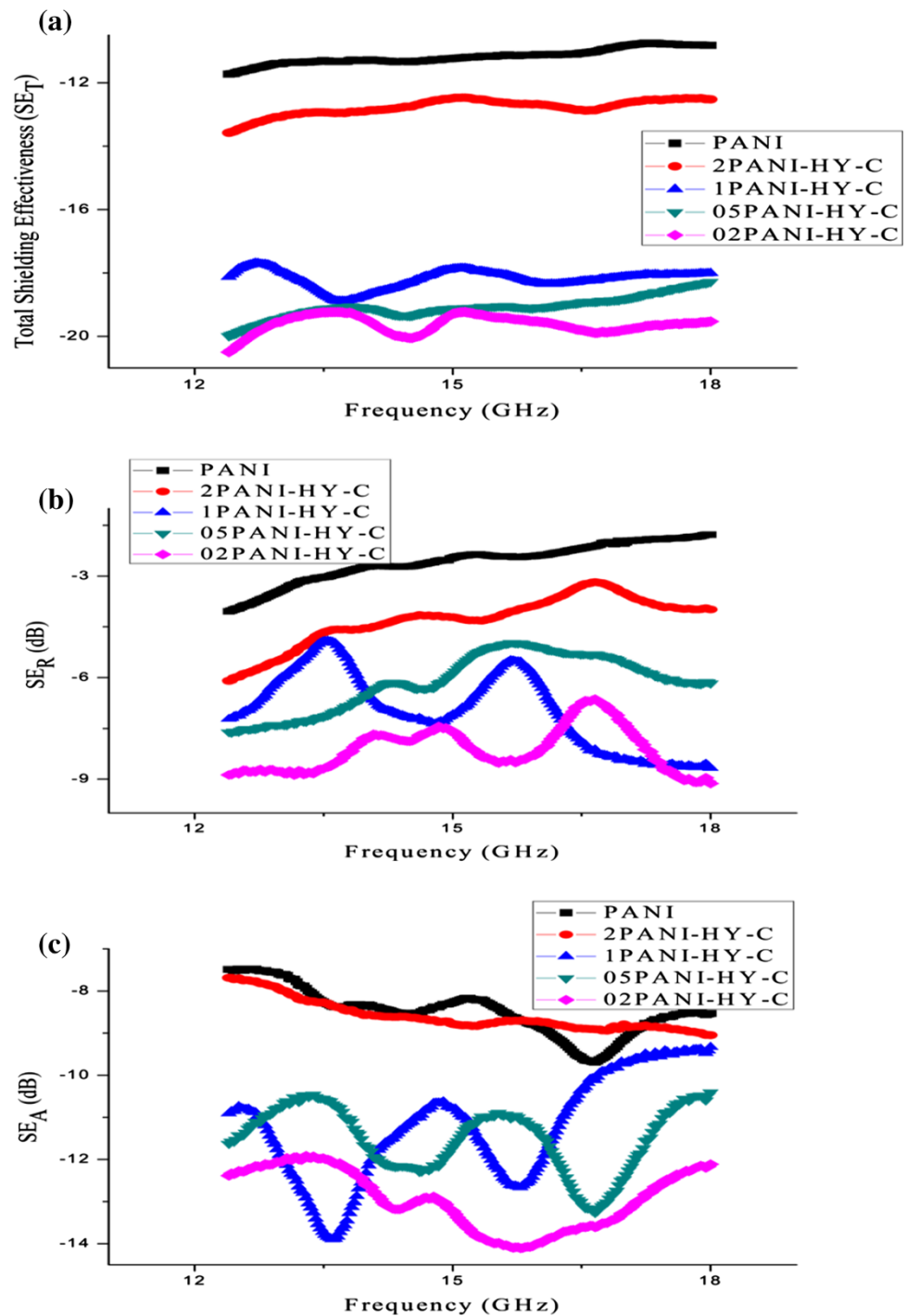
where SE_R , SE_A and SE_M are shielding effectiveness due to reflection, absorption and multiple reflections, respectively. The scattering parameters S_{11} (or S_{22}) and S_{21} (or S_{12}) of a two-port network analyzer can be related with reflectance and transmittance as

$$T = \left| \frac{E_T}{E_I} \right|^2 = |S_{21}|^2 = |S_{12}|^2 \quad (3)$$

$$R = \left| \frac{E_R}{E_I} \right|^2 = |S_{11}|^2 = |S_{22}|^2 \quad (4)$$

The absorbance (A) can be written as: $A = (1 - R - T)$ (5)

Fig. 7 Plot of **a** total shielding effectiveness, **b** SE_R and **c** SE_A of PANI and composites



Here, it should be noted that the absorption coefficient is given with respect to the power of the incident EM wave. When SE_A is ≥ 10 dB, SE_M is negligible (Singh et al. 2013; Das et al. 2000). Therefore, third term in Eq. 2 (i.e. SE_M) vanishes and SE_T can be conveniently expressed as

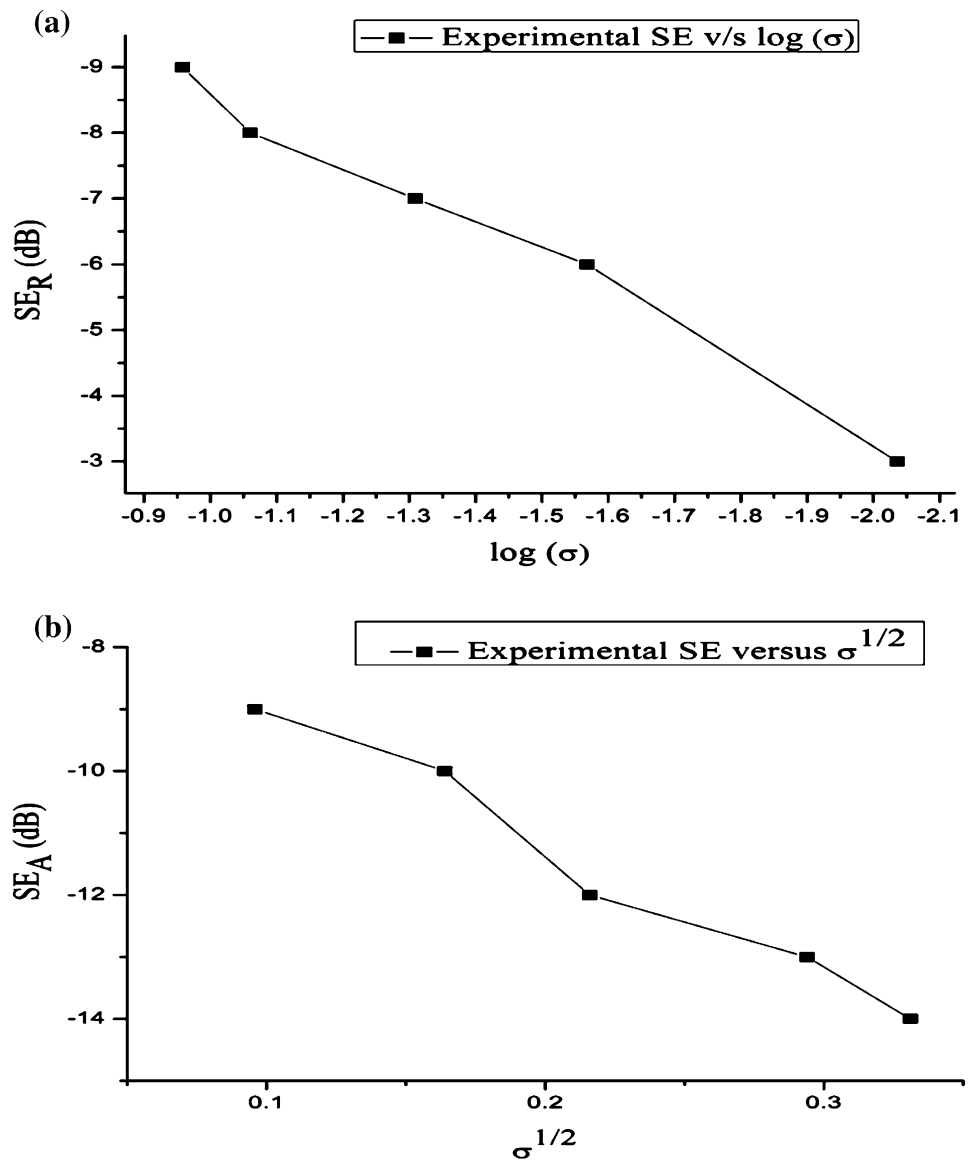
$$SE_T = SE_R + SE_A \tag{6}$$

Further, the relative intensity of the effectively incident EM wave inside the materials after first reflection is based

on the quantity $(1 - R)$. The effective absorbance (A_{eff}) can be described as $A_{eff} = (1 - R - T)/(1 - R)$ after normalization with respect to the power of the effectively incident EM wave inside the shielding material. Therefore, it is convenient to express the reflection and effective absorption losses in the form of $-10 \log(1 - R)$ and $-10 \log(1 - A_{eff})$, respectively (Singh et al. 2013), i.e.

$$SE_R = 10 \log(1 - R) \tag{7}$$

Fig. 8 Plot of **a** SE_R versus $\log(\sigma)$ and **b** SE_A versus $\sigma^{1/2}$ of PANI and composites



$$SE_A = 10 \log(1 - A_{\text{eff}}) = 10 \log \frac{T}{1 - R} \tag{8}$$

The term skin depth (δ) is the depth of penetration at which the intensity of the electromagnetic wave is reduced to $1/e$ of its original strength. The δ is dependent upon various parameters like angular frequency (ω), real relative permeability (μ') and total conductivity (σ_T) and can be expressed as

$$\delta = \sqrt{2/\omega\mu\sigma_T}. \tag{9}$$

Therefore, at any given frequency, skin depth decreases with the increase in both magnetic permeability as well as electrical conductivity. Further, for an electrically thick shield ($t > \delta$), frequency (ω) dependence of far field reflection and absorption losses can be expressed in the

terms of total conductivity (σ_T) real permeability (μ'), skin depth (δ) and thickness (t) of the shield material as

$$SE_R \text{ (dB)} = -10 \log \left(\frac{\sigma_T}{16\omega\epsilon_0\mu'} \right) \tag{10}$$

$$SE_A \text{ (dB)} = -20 \frac{t}{\delta} \log e = -8.68 \left(\frac{t}{\delta} \right) \tag{11}$$

The σ_T and δ can be related to imaginary permittivity (ϵ'') and real permeability (μ') as $\sigma_T = \omega\epsilon_0\epsilon''$

$$\delta = \left(\frac{2}{\sigma_T\omega\mu'} \right)^{\frac{1}{2}} \tag{12}$$

This gives absorption loss as

$$SE_A \text{ (dB)} = -8.68t \left(\frac{\sigma_T\omega\mu'}{2} \right)^{\frac{1}{2}} \tag{13}$$

The shallow skin depths and high conductivity (σ_T) values in the microwave region often result in contribution of SE_A becoming much more compared to SE_R . Therefore, absorption acts as dominant shielding mechanism with nominal reflection values.

Figure 7 illustrates the plot of (a) total shielding effectiveness, (b) SE_R and (c) SE_A of PANI and composites. The lowest monomer content composite 02PANI-HY-C (0.02 M) shows best shielding effectiveness of 21 dB, thus indicating that the lowest content leads to the formation of thinnest polymeric film over hybrid carbon assemblage and leads to reduction in contact resistance between hybrid carbon assemblage and polyaniline phases, respectively. Hence, 02PANI-HY-C exhibits highest conductivity and shielding effectiveness. Figure 7b shows that reflection loss increases slightly from -3.0 to -9.0 dB with the decrease aniline monomer content. Also, variation of loss tangent with decrease in molar level of aniline may be ascribed to increase in the conductivity of composites (Fig. 6). The absorption loss (Fig. 7c) exhibits rapid enhancement from -9.0 to -14.0 dB with the increased conductivity. This may be explained in terms of increase in conductivity as well as capacitive coupling effects. From Eq. (12) it is seen that increasing conductivity leads to corresponding decrease in skin depth which may be helpful in designing thinner EMI shields. The plot of SE_R (dB) versus $\log(\sigma)$ (Fig. 8a) and SE_A (dB) versus $(\sigma)^{1/2}$ (Fig. 8b) shows linear dependence over conductivity and confirming the validity of Eqs. (10) and (13). Further it is predicted that the increased conductivity may manifest itself as increase in both long range charge transport as well as number of possible relaxation modes, leading to enhanced ohmic losses in the proposed electromagnetic shielding material (Phang et al. 2008; Saini et al. 2009). The total shielding effectiveness of -21 dB indicates that these materials could be utilized effectively for the shielding purposes in the Ku-band (12.4–18.0 GHz).

Conclusion

The PANI films have been successfully grown over three-dimensional hybrid carbon assemblage substrate. The UV-vis, FTIR and XRD show systematic shifting in the positions of characteristic bands and peaks of PANI, indicative of significant interactions between the hybrid carbon assemblage and PANI. SEM studies show that at higher concentrations, PANI tends to polymerize upon itself leading to globular agglomerates and poor adhesion films. The high electrical conductivity of 0.11 S cm^{-1} in 02PANI-HY-C has been ascribed to the synergistic effect of two complementing phases (PANI and Hybrid carbon assemblage). The total shielding effectiveness of 21 dB

indicates that these materials could be utilized effectively in the Ku-band (12.4–18.0 GHz) and are suitable to be used in EMI shielding devices.

Acknowledgments The authors are thankful to the TDT Division of Department of Science and Technology, Government of India, for providing financial assistance in the form of major research project.

Open Access This article is distributed under the terms of the Creative Commons Attribution License which permits any use, distribution, and reproduction in any medium, provided the original author(s) and the source are credited.

References

- Das TK, Prusty S (2013) Graphene based Polymer composites and their applications. *Polym-Plast Technol Eng* 52:319–331
- Das NC, Khastgir D, Chaki TK, Chakraborty A (2000) Electromagnetic interference shielding effectiveness of carbon black and carbon fibre filled EVA and NR based composites. *Composites A* 31:1069–1081
- Gupta TK, Singh BP, Mathur RB, Dhakate SR (2014) Multiwalled carbon nanotube-graphene-polyaniline multiphase nanocomposites with superior electromagnetic shielding effectiveness. *Nanoscale* 6:842–851
- Iijima S, Ichihashi T (1993) Single-shell carbon nanotubes of 1-nm diameter. *Nature* 363:603–605
- Jimeno A, Goyanes S, Eceiza A, Kortaberria G, Mondragon I, Corcuera MA (2009) Effects of amine molecular structure on carbon nanotubes functionalization. *J Nanosci. Nanotechnol.* 9:1–6
- Meyer JC, Geim AK, Katsnelson MI, Novoselov KS, Booth TJ, Roth S (2007) The structure of suspended graphene sheets. *Nature* 446:60–63
- Novoselov KS, Jiang D, Booth T, Khotkevich VV, Morozov SV, Geim AK (2005) Two dimensional atomic crystals. *PNAS* 102:10451–10453
- Olmedo L, Hourquebie P, Jousse F (2001) In: Nalwa HS (ed) *Handbook of organic conductive molecules and polymers*. Wiley, Chichester, p 367
- Ozkazanca E, Zorb S, Ozkazancb H, Yuksel Guneya H, Abacia U (2012) Synthesis, characterization and dielectric behavior of (ES)-form polyaniline/cerium(III)-nitrate-hexahydrate composites. *Mater Chem Phys* 133:356–362
- Pande S, Singh BP, Mathur RB, Dhama TL, Saini P, Dhawan SK (2009) Improved electromagnetic interference shielding properties of MWCNT-PMMA composites using layered structures. *Nanoscale Res Lett* 4:327–334
- Phang SW, Tadokoro M, Watanabe J, Kuramoto N (2008) Synthesis, characterization and microwave absorption property of doped polyaniline nanocomposites containing TiO₂ nanoparticles and carbon nanotubes. *Synth Met* 158:251–258
- Qin FX, Peng HX, Pankratov N, Phan MH, Panina LV, Ipatov M, Zhukova V, Zhukov A, Gonzalez J (2010) Exceptional electromagnetic interference shielding properties of ferromagnetic microwires enabled polymer composites. *J App Phys* 108: 044510
- Saini P, Choudhary V, Singh BP, Mathur RB, Dhawan SK (2009) Polyaniline-MWCNT nanocomposites for microwave absorption and EMI shielding. *Mater Chem Phys* 113:919–926
- Saini P, Choudhary V, Singh BP, Mathur RB, Dhawan SK (2011) Enhanced microwave absorption behavior of polyaniline-CNT/

- polystyrene blend in 12.4–18.0 GHz range. *Synth Met* 161:1522–1526
- Sharma K, Shukla M (2013) Three-phase carbon fiber amine functionalized carbon nanotubes epoxy composite: processing, characterisation, and multiscale modeling. *J Nanomater*. doi:[10.1155/2014/837492](https://doi.org/10.1155/2014/837492) (article ID 837492)
- Sharma AK, Sharma Y (2012) Pseudo capacitive studies of Polyaniline-carbon nanotubes composite as electrode material for supercapacitor. *Anal Lett* 45:2075–2085
- Singh BP, Prabha SP, Gupta T, Garg P, Kumar G, Pande I, Pande S, Seth RK, Dhawan SK, Mathur RB (2011) Designing of multi-walled carbon nanotubes reinforced low density polyethylene nanocomposites for suppression of electromagnetic radiation. *J Nanopart Res* 13:7065–7074
- Singh BP, Bhardwaj P, Choudhary V, Mathur RB (2013) Enhanced microwave shielding and mechanical properties of multiwall carbon nanotubes anchored carbon fiber felt reinforced epoxy multiscale composites. *Appl Nanosci*. doi:[10.1007/s13204-013-0214-0](https://doi.org/10.1007/s13204-013-0214-0)
- Yang K, Gu MY, Guo YP, Pan XF, Mu GH (2009) Effects of carbon nanotube functionalization on the mechanical and thermal properties of epoxy composites. *Carbon* 47:1723–1737